

Global Ductility Demands of RC Frames with Various Post-Yield Stiffness Ratio and Ductility Capacity Ratio Under Near-Field Earthquakes

A Faisal^{1,3}, F V Riza¹, B Hadibroto²

¹Program Studi Teknik Sipil, Fakultas Teknik, Universitas Muhammadiyah Sumatera Utara, Medan, Indonesia

²Civil Engineering Programme, Faculty of Engineering, State University of Medan, Indonesia

³Email: adef@umsu.ac.id

Abstract. The directivity pulse motion in near-field earthquake affects the responses of structures. The response includes the roof drifts and interstory drifts, which is so-called the ductility demand. Although many studies have done in this topic, the effect of various post-yield stiffness ratio and ductility capacity ratio to the global ductility demands of reinforced concrete (RC) frames under near-field ground motion is not specifically investigated yet. The trend of global ductility demands of RC frames under near-field earthquake is the objective of this study. The frames are modeled with various fundamental period, behavior factor, plastic rotation capacity, post-yield stiffness ratio, and ductility capacity ratio. The study reveals that the effect of ductility capacity ratio on the global ductility demands is apparent as the plastic rotation capacity changes. The global ductility demand is also found influenced by global post-yield stiffness ratio and behaviour factor.

1. Introduction

Many studies show that inelastic demands of structures depend on the type of induced ground motion (e.g. far-field and near-field ground motions). The parameters governed the near-field ground motions (NFGM) and its effect on the inelastic demand of structures have been extensively studied. In the 1970s, a pioneering work in investigating NFGM affecting a building was conducted by Bertero et al. [1]. The effect of NFGM on the structural response is further explored by Hall et al. [2]. The study found that the effect of NFGM can be very effective in causing damage in structure when the fundamental period of vibration of structure is comparable to the duration of the NFGM's pulse. Maholtra [3] found the directivity pulse motion affected the responses of structures in increasing the base shear and interstory drifts in high-rise buildings, increasing the ductility demand. Alavi and Krawinkler [4], Krawinkler et al. [5], and Krawinkler et al. [6] revealed that large elastic storey shear forces in the upper storey of the structure were found to be generated by FDE with a fundamental period of the structure higher than the pulse period.

Using the real records of forward directivity earthquake (FDE), similar studies were conducted by Akkar et al. [7] and Kalkan and Kunnath [8] in exploring the response of generic multi-storey structures due to FDE and their results support previous findings [4]. Approximately, similar findings were also reported in some studies which were using generic shear frame models induced by real and synthetic FDEs [9]. Majid et al. [10] employed the real NFGM and far-field ground motion in evaluating the response of irregular

RC frames. The response showed that NFGM produced higher drift compared with far-field ground motion. The response of the 4- to 18-storey RC framed structures under single and sequential near-field earthquakes conducted by Zahid et al. [11] and Faisal et al. [12] in order to identify its displacement ductility and storey ductility demand. Beiraghi et al. [13] investigated the seismic behavior of the 20-story, 30-story and 40-story of core-wall buildings with fixed bases subjected to NFGM with respect to the energy concepts.

Although many studies have done in the topic of effect of NFGM on the response of buildings, the relation of post-yield stiffness ratio and ductility capacity ratio to the global ductility demands of building under NFGM is not specifically investigated yet. Therefore this study aims to indentify the trend of global ductility demands of RC frames under FDE. The demands is explored in the perspective of global post-yield stiffness ratio and global ductility capacity ratio. The study employs various fundamental periods of structures, behavior factors, and plastic rotation capacities in order to achieve a general insight.

2. Methods

2.1. Inelastic Structural Models

2.1.1. Properties of the Model. The generic frame model used in this study is proposed by Faisal et al. [12]. It focuses on the regular geometric system and horizontal dimension of the system in any story is <130% of an adjacent story or no setback. Considered fundamental periods of the 3D generic MDOF model are $T_1 = 0.45, 0.75, 1.26,$ and 1.71 seconds. The elevation and plan of 3D generic MDOF structure is as shown in Figure 1. The model is assumed to be built in Zone III in Greece with spectra design (Figure 2). Columns and beams at each story have the same stiffness in order to reduce the uncertainty in modelling. The plan shape of floor and roof is squared plan size, $H_i \times H_i$. By assuming ratio of the span to story height is equal to 2.0 for all stories of the generic model hence parameter H_i is equal to the twice of column height.

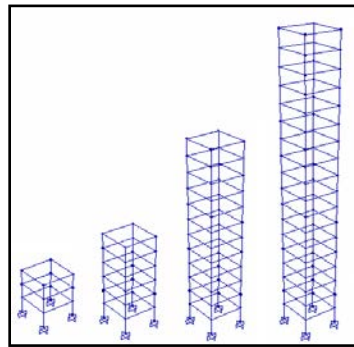


Figure 1. Models of 3D generic 3, 6, 12, and 18-story single-bay frames [12]

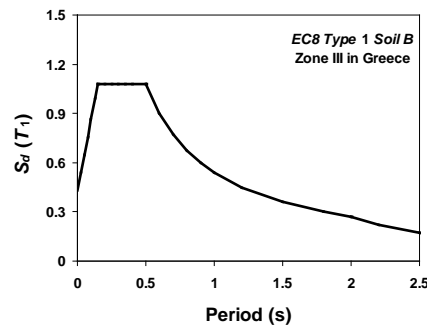


Figure 2. Design response spectrum of Eurocode 8 for Type 1 and Soil B at Zone III of Greece

2.1.2. Weight and Stiffness. The story weight of RC structure is assumed to be identical (1240 kN) at all stories and all models, whereas stiffness is assumed to be the same for every 3 levels (stepwise distribution). The models are set up to be as the fundamental period of model increases the beam-to-column stiffness ratio decreases. The model sets to behave dominantly in flexure as the fundamental period (or number of story) increase.

2.1.3. Seismic Design and Strength. The seismic base shear is defined from ordinate design spectrum at period T_1 of Type 1 spectrum of Eurocode 8 for condition of Soil B with peak ground acceleration (PGA), $a_g=0.36$ g, as shown in Figure 2. The a_g is based on 475-years return period of earthquake that reflecting the condition of Seismic Zone III at Greece. Greece represents the highest seismic region in Europe, along with Turkey and Italy, whereas Zone III is the highest seismic zone in Greece. The moment and rotation of this linear elastic static analysis at $q = 1$ means that both result from the same elastic and yield

forces, $F_e = F_y$. The bending moment of member at this stage is considered as the yield strength of member.

2.1.4. Plastic Hinge and Rotation Capacity. The plastic hinge is represented by moment-rotation relationship, whereas the shear deformation as well as moment-axial interaction are disregarded. The plastic hinge is modelled using lumped plasticity model. To simulate the cyclic behavior of members in plastic hinge under load reversals, Modified-Takeda hysteresis rule is employed. The unloading and reloading parameters (α and β) in hysteresis rule for beam member are equal to 0.3 and 0.6 respectively. This study employs the rotation capacities represent the capacity of general RC structures.

2.1.5. Ground Motion. Selected ground motions for FDE are presented in Table 5 sourced from seismic station built in stiff soil. FDE motions are dominated by California and Taiwan earthquakes and mainly from source-to-site distance less than 10 km and magnitude larger than M6.0. The scaling factor of selected ground motions used in the study is corresponding to the fundamental period of models.

Table 5. Selected FDE motions on the stiff soil from PEER-NGA

No.	Date	Earthquake Name	Mag. (Mw)	Closest Dist. (km)	Station
1	24/04/1984	Morgan Hill	6.2	0.53	Coyote Lake Dam (SW Abut)
2	18/10/1989	Loma Prieta	6.9	9.96	Gilroy - Gavilan Coll.
3	18/10/1989	Loma Prieta	6.9	3.88	LGPC
4	28/06/1992	Landers	7.3	2.19	Lucerne
5	17/01/1994	Northridge-01	6.7	5.43	Jensen Filter Plant
6	17/01/1994	Northridge-01	6.7	5.43	Jensen Filter Plant Generator
7	17/01/1994	Northridge-01	6.7	5.19	Sylmar - Converter Sta East
8	17/01/1994	Northridge-01	6.7	5.30	Sylmar - Olive View Med FF
9	17/08/1999	Kocaeli, Turkey	7.5	10.92	Gebze
10	20/09/1999	Chi-Chi, Taiwan	7.6	3.14	CHY028
11	20/09/1999	Chi-Chi, Taiwan	7.6	3.78	TCU049
12	20/09/1999	Chi-Chi, Taiwan	7.6	0.66	TCU052
13	20/09/1999	Chi-Chi, Taiwan	7.6	5.97	TCU053
14	20/09/1999	Chi-Chi, Taiwan	7.6	5.30	TCU054
15	20/09/1999	Chi-Chi, Taiwan	7.6	0.32	TCU068
16	20/09/1999	Chi-Chi, Taiwan	7.6	0.91	TCU075
17	20/09/1999	Chi-Chi, Taiwan	7.6	2.76	TCU076
18	20/09/1999	Chi-Chi, Taiwan	7.6	5.18	TCU082
19	20/09/1999	Chi-Chi, Taiwan	7.6	1.51	TCU102
20	20/09/1999	Chi-Chi, Taiwan	7.6	6.10	TCU103

2.1.6. Global Ductility and Post-Yield Stiffness Ratio Capacities. The ductility and post-yield stiffness ratio are resulted from nonlinear static analysis or pushover analysis [12]. To relate the global ductility capacity with the story ductility capacity, the ratio of story ductility and global ductility capacities is employed in the study and denoted as \mathcal{G}_c . The ratio is defined based on the regression analysis in polynomial fourth-order form. The relationship of \mathcal{G}_c with number of story (N) for $0.45 \leq T_1 \leq 1.71$ s is in the following formula ($R^2 = 0.977$):

$$\mathcal{G}_c = 6.177T_1^3 - 17.543T_1^2 + 16.450T_1 - 3.210 \quad (1)$$

The parameter of ratio of global post-yield stiffness to elastic stiffness, r_K , to represents global stiffness of the structures [12] is used in this study. The relationship of r_K as a function of the fundamental period of vibration, T_1 , behavior factor, q , and plastic rotation capacity, θ_p , of the system ($R^2 = 0.925$ and Sig.F-ratio ≈ 0.00) is as follow:

$$\text{Log}(r_K) = -0.508T_1 - 0.135q - 11.252\theta_p - 0.952 \quad (2)$$

3.Result and Discussion

3.1. Effect of Global Ductility Capacity Ratio

The ratio of maximum story ductility to roof ductility denotes global ductility capacity ratio, \mathcal{G}_c . Figure 3 showshow global ductility capacity ratio under two types of plastic rotation capacity (Rot.=0.02 and 0.06) affects the roof ductility demand in logarithmic form. This figure also reflects the fundamental period of models under consideration in its each point of post-yield stiffness ratio. Although \mathcal{G}_c is apparent in influencing μ_{Δ} , the trend of how \mathcal{G}_c governed μ_{Δ} is not clear as the plastic rotation capacity changes. It seems other factor also plays an important role to this trend, e.g. fundamental period of vibration, T_1 . In statistical analysis point of view, the effect of \mathcal{G}_c on the roof ductility demand was found about similar with the effect of T_1 . Therefore, the effect of \mathcal{G}_c on the roof ductility demand might be has dependency to T_1 .

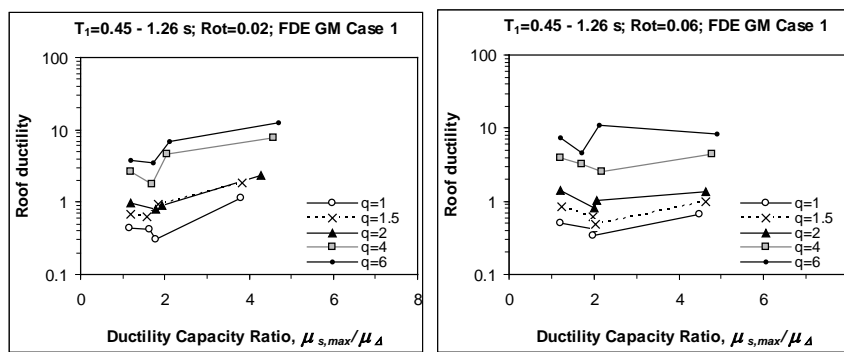


Figure 3. Mean roof ductility demand as a function of ductility capacity ratio and behavior factor. Each point represents fundamental period of models $T_1 = 0.45, 0.75, 1.26$ and 1.71 s.

3.2. Effect of Global Post-Yield Stiffness Ratio

Effect of global post-yield stiffness ratio, r_K , on the roof ductility demand, μ_{Δ} , can be seen in Figure 4. This figure explains the roof ductility demand as a function of global post-yield stiffness ratio and plastic rotation capacity (denotes Rot.=0.02, 0.04, and 0.06). It demonstrates that the post-yield stiffness ratio decreases as the roof ductility demand increases. This mechanism is correct because when the fundamental period of system under the same strength increases, the global stiffness decreases (more flexible), hence roof and story drifts increases. In Figure 4, each point of post-yield stiffness ratio also represents a behavior factor of the system, which explains the change in ductility class (e.g. DCM to DCH in Eurocode 8) affects the post-yield stiffness and thus it influences the roof ductility demand due to its post-yield stiffness ratio.

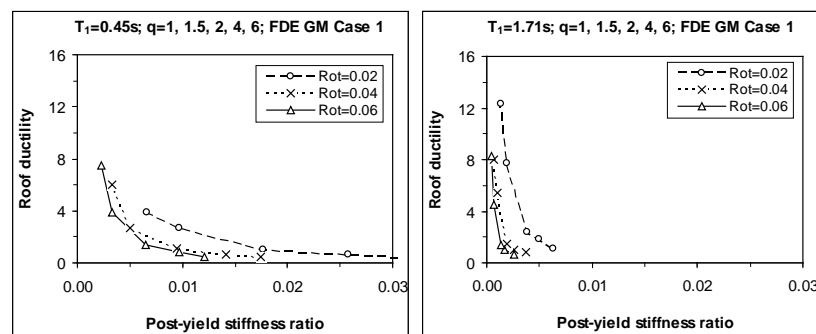


Figure 4. Mean roof ductility demand of models with $T_1 = 0.45$ and 1.71 s as a function of global post-yield stiffness ratio and plastic rotation capacity. Each point represents a behavior factor.

Figure 5 depicts the of ductility demand as a function of global post-yield stiffness ratio and behavior factor for two types of plastic rotation capacity (Rot.=0.02 and 0.06). Each point in this figure represents fundamental period of models under consideration and hence the trend follows the same way as previously discussed. It is evident that no regular trend is demonstrated as the post-yield stiffness ratio is changed. In this case, the irregularity of effect post-yield stiffness ratio on the roof ductility demand explains its dependency to fundamental period since its shape of line indicates the same trend as in Figure 5. In general, effect of behavior factor on the trend of roof ductility demand in Figure 5 is superior to the effect of post-yield stiffness ratio.

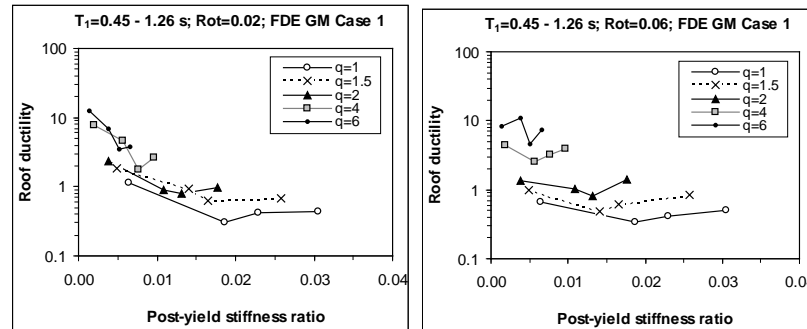


Figure 5. Mean roof ductility demand as a function of global post-yield stiffness ratio and behavior factor. Each point represents fundamental period of models $T_1 = 0.45, 0.75, 1.26$ and 1.71 s.

It should be noted that the variation of post-yield stiffness ratio of the system under the same behavior factor or ductility class is reflecting the variation of strength (i.e. flexural strength) of the elements represented by the ratio of maximum bending moment to the yield moment (M_c/M_y). It is because the M_c/M_y of elements has involved in the formation of the backbone curve of the hysteresis system, which in turn has participated in the global backbone curve. Unfortunately, the effect of M_c/M_y on the roof ductility ratio could not be presented since this parameter was not varied in designing the model. However, the variation of post-yield stiffness ratio in this study could reflect the variation of M_c/M_y by assuming a single value of plastic rotation capacity is used. Therefore, it can be said that as the M_c/M_y of element in the system under the same plastic rotation capacity increases, the post-yield stiffness ratio increases and hence the roof ductility demand decreases.

4. Conclusions

This study investigates the global ductility demands of RC frames with various post-yield stiffness ratio and ductility capacity ratio under forward directivity motion of near-field earthquake. The models include the various fundamental period, behavior factor, and plastic rotation capacity. The following conclusions can be drawn from the study:

1. As the plastic rotation capacity changes, the effect of ductility capacity ratio on the global ductility demands is clearly apparent.
2. The change in ductility class (e.g. DCM to DCH in Eurocode 8) affects the post-yield stiffness and thus it influences the roof ductility demand due to its post-yield stiffness ratio.

Acknowledgement

Support for this project was provided by the Grant of Penelitian dan Pengabdian Kepada Masyarakat Internal UMSU tahun 2016.

References

- [1] Bertero, V.V., Mahin, S.A. and Herrera, R.A., 1978. Aseismic design implications of near-fault San Fernando earthquake records. *Earthquake engineering & structural dynamics*, 6(1), pp.31-42.
- [2] Hall, J.F., Heaton, T.H., Halling, M.W. and Wald, D.J., 1995. Near-source ground motion and its effects on flexible buildings. *Earthquake spectra*, 11(4), pp.569-605.
- [3] Malhotra, P.K., 1999. Response of buildings to near-field pulse-like ground motions. *Earthquake Engineering and Structural Dynamics*, 28(11), pp.1309-1326.
- [4] Alavi, B. and Krawinkler, H., 2001. *Effects of near-fault ground motions on frame structures*. Stanford: John A. Blume Earthquake Engineering Center.
- [5] Krawinkler, H., Medina, R. and Alavi, B., 2003. Seismic drift and ductility demands and their dependence on ground motions. *Engineering structures*, 25(5), pp.637-653.
- [6] Krawinkler, H., Alavi, B. and Zareian, F., 2005. Impact of near-fault pulses on engineering design. *Direction in Strong Motion Instrumentation*, 58(1), pp.83-106.
- [7] Akkar, S., Yazgan, U. and Gülkan, P., 2005. Drift estimates in frame buildings subjected to near-fault ground motions. *Journal of Structural Engineering*, 131(7), pp.1014-1024.
- [8] Kalkan, E. and Kunnath, S.K., 2006. Effects of fling step and forward directivity on seismic response of buildings. *Earthquake spectra*, 22(2), pp.367-390.
- [9] Sehhati, R., Rodriguez-Marek, A., ElGawady, M. and Cofer, W.F., 2011. Effects of near-fault ground motions and equivalent pulses on multi-story structures. *Engineering Structures*, 33(3), pp.767-779.
- [10] Majid, T.A., Wan, H.W., Zaini, S.S., Faisal, A. and Wong, Z.M., 2010. The effect of ground motion on non-linear performance of asymmetrical reinforced concrete frames. *Disaster Advances*, 3(4), pp.35-39.
- [11] Zahid, M.Z.A.M., Majid, T.A. and Faisal, A., 2012. Effect Of Repeated Near Field Earthquake To The High-Rise Rc Building. *Australian Journal of Basic and Applied Sciences*, 6(10), pp.129-138.
- [12] Faisal, A., Majid, T.A. and Hatzigeorgiou, G.D., 2013. Investigation of story ductility demands of inelastic concrete frames subjected to repeated earthquakes. *Soil Dynamics and Earthquake Engineering*, 44, pp.42-53.
- [13] Beiraghi, H., Kheyroddin, A. and Kafi, M.A., 2016. Forward directivity near-fault and far-fault ground motion effects on the behavior of reinforced concrete wall tall buildings with one and more plastic hinges. *The Structural Design of Tall and Special Buildings*, 25(11), pp.519-539.
- [14] ASCE. (2005). *Minimum design loads for buildings and other structures*, ASCE/SEI 7-05. Reston, VA.: ASCE.
- [15] CEN. (2004). *Eurocode 8: Design of structures for earthquake resistance. Part 1: General rules, seismic actions and rules for buildings* (Vol. 1). Brussels.: European Committee for Standardization.